

**SPIE Proceeding 2006**

## Ex-plant retinal laser induced threshold studies in the millisecond time regime

K. Schulmeister, J. Husinsky, B. Seiser, F. Edthofer, H. Tuschl and D. J. Lund

Please **register** to receive our ***Laser, LED & Lamp Safety* NEWSLETTER**  
(about 4 times a year) with information on new downloads:  
<http://laser-led-lamp-safety.seibersdorf-laboratories.at/newsletter>

This paper can be downloaded from <http://laser-led-lamp-safety.seibersdorf-laboratories.at>

Karl Schulmeister, Johannes Husinsky, Bernhard Seiser, Florian Edthofer, Helga Tuschl and David J. Lund, "Ex-plant retinal laser induced threshold studies in the millisecond time regime", Optical Interactions with Tissue and Cells XVII, Steven L. Jacques and William P. Roach, Editors, Proc. SPIE Vol. 6084 (2006), doi:10.1117/12.662811

Copyright 2006 Society of Photo-Optical Instrumentation Engineers. One print or electronic copy may be made for personal use only. Systematic electronic or print reproduction and distribution, duplication of any material in this paper for a fee or for commercial purposes, or modification of the content of the paper are prohibited.

# ***Optical Interactions with Tissue and Cells XVII***

**Steven L. Jacques**  
**William P. Roach**  
*Editors*

**21. January 2006**  
**San Jose, USA**

*Sponsored by*  
U.S. Air Force Office of Scientific Research  
SPIE – The International Society for Optical Engineering

**Proceedings of SPIE**  
**Volume 6084**

# Ex-plant retinal laser induced threshold studies in the millisecond time regime

Karl Schulmeister<sup>\*</sup>, Johannes Husinsky<sup>1</sup>, Bernhard Seiser<sup>1</sup>, Florian Edthofer<sup>1</sup>, Helga Tuschl<sup>2</sup> and David J. Lund<sup>3</sup>

<sup>1</sup> ARC Seibersdorf research, Laser and optical radiation test lab, A-2444 Seibersdorf, Austria

<sup>2</sup> ARC Seibersdorf research, Toxicology Department, A-2444 Seibersdorf, Austria

<sup>3</sup> U.S. Army Medical Research Detachment, Walter Reed Army Institute of Research  
7965 Dave Erwin Drive, Brooks City-Base, TX 78235-5108

## ABSTRACT

Excised bovine retinas were used as model for threshold determination of laser induced thermal damage in the pulse regime of 1 ms to 655 ms for a range of laser spot size diameters. The thresholds as determined by fluorescence viability staining compare very well with the prediction of thermal damage models. Both models compare well with published and new Rhesus monkey threshold data. A distinctive dependence of the threshold on laser spot size diameter for different pulse duration was found which indicates that current (ICNIRP, ANSI and IEC) laser exposure limits for large spots can be increased in this pulse duration regime. A time dependent  $\alpha_{\max}$  is proposed which only for the case of long exposure durations has the current value of 100 mrad, but decreases to smaller angles for short exposure durations, effectively increasing the permissible exposure level. An explanation based on intra-retinal scattering is offered for the unexpected spot size dependence for spot diameters less than about 80  $\mu\text{m}$ . The time dependence and nature of damage is discussed for pulse durations shorter than 1 ms where bubble induced damage seems to lead to a threshold a factor of 10 lower than the thermally induced threshold, resulting in the need to lower the MPE values for this condition. Possible changes of the MPE values are offered and discussed.

**Keywords:** laser safety, hazard analysis, computer model, bovine model, apparent source, retinal thermal injury, MPE, IEC 60825-1, ANSI Z136.1

## 1. INTRODUCTION

Exposure limits (EL) for laser radiation are set on the international level by ICNIRP [1]. These exposure limits are adopted by IEC and published in IEC 60825-1 [2] and IEC 60825-14 [3], where the exposure limits are referred to as maximum permissible exposure (MPE). ANSI also sets MPEs for laser radiation in ANSI Z136.1 [4] on a US national basis, however, these are usually identical with ICNIRP ELs. Current exposure limits are based on experimental animal damage threshold data. For exposure limits for the retina, rhesus monkey data has been so far the model of choice for determining laser induced damage threshold values [5]. Results of computer models and of *in vitro* threshold experiments were considered to be very limited in its applicability to serve as model for the determination of absolute threshold levels which can be related directly to the human case. We report on the results of computer models and of a bovine *in vitro* (explant) model which were validated against rhesus monkey data. The models appropriately predict absolute damage threshold values in the wavelength and pulse duration range under consideration, namely the visible wavelength range and pulse durations from 1 ms to 1 s. The data, for the first time, provide for a complete understanding of the spot size dependence of retinal thermal damage thresholds in the visible wavelength range, which can be the basis for improving the accuracy of both laser and broadband retinal thermal MPEs<sup>1</sup>.

---

\* [karl.schulmeister@arcs.ac.at](mailto:karl.schulmeister@arcs.ac.at) [www.healthphysics.at/laser\\_e](http://www.healthphysics.at/laser_e)

<sup>1</sup> In the following, for simplicity, we limit the discussion to *laser* exposure limits, however, the spot size dependence of damage thresholds and exposure limits on retinal image size also directly relates to broadband incoherent radiation.

### 1.1. Corneal and retinal ‘space’

Current laser exposure limit guidelines and standards define the retinal spot size dependence of the MPE values for thermal damage of the retina in terms of a multiplication factor in the MPEs, that varies the values of the MPE relative to the MPE value for the assumed minimal retinal spot size. For minimal spot sizes, the MPE is the smallest and the factor ( $C_6$  for IEC and  $C_E$  for ICNIRP and ANSI) equals unity. The MPEs are defined at the cornea, even for wavelength ranges where the injury occurs at the retina, since the exposure levels at the retina can not be determined directly. For a safety analysis, exposure levels (radiant exposure or irradiance) at the cornea (averaged over the area of a 7 mm aperture) are compared to the MPE value, which is either given in units of  $J\ m^{-2}$  or  $W\ m^{-2}$  [6]. By multiplying the average radiant exposure at the cornea with the area of the 7 mm aperture, a value in terms of energy (or power) is obtained that passes through the 7 mm aperture, which is equivalent to what in experimental threshold studies is referred to as the ‘total intraocular energy’, TIE. When the MPE is also multiplied with the area of the 7 mm aperture, a comparison of this value (now given in Joules or Watts) with the TIE is equivalent to comparing the averaged radiant exposure with the MPE. The energy per pulse that is incident on the retina can be calculated by multiplying the TIE with the transmittance of the ocular media in front of the retina. The retinal radiant exposure in units of  $J\ m^{-2}$  can be calculated from this value by division with the area over which the energy that is incident on the retina is distributed. The dependence of the MPE on the retinal spot size is given in terms of ‘the angular subtense of the apparent source’ (symbol:  $\alpha$ ) which characterises the angle that the retinal irradiance pattern subtends at the corresponding principle plane of the cornea-lens system of the eye (see [7] for a more detailed discussion on the apparent source). For a human, the retinal spot diameter  $d_r$  in units of  $\mu m$  is related to the angular subtense of the spot  $\alpha$  in units of mrad by  $d_r = \alpha\ 17\ mm$ , where the air-equivalent distance from the retina to the corresponding principle plane of the human eye is used (for the rhesus monkey eye, the corresponding distance is 13.5 mm. Thus, for a top hat profile<sup>2</sup> that subtends an angular subtense of  $\alpha$ , the area of the retinal spot is directly proportional to  $\alpha^2$  and the retinal radiant exposure is directly proportional to  $TIE/\alpha^2$ .

With these relationships it is possible to discuss the spot size dependence (as a function of retinal spot diameter and pulse duration) of the retinal thermal damage either in ‘retinal space’, i.e. by analysing the damage threshold in terms of retinal radiant exposure (with units of  $J\ m^{-2}$ ) or in ‘corneal space’ where the threshold for retinal damage is specified in terms of the TIE (with units of  $J$  or  $\mu J$ ) which can also be compared to the MPE multiplied with the area of the 7 mm diameter averaging aperture.

### 1.2. Current dependence on retinal spot size ( $\alpha$ )

The angular subtense of the smallest spot size that can be optically achieved at the retina is referred to as the ‘*minimum angular subtense*’ and has the symbol  $\alpha_{min}$ . The minimum angular subtense  $\alpha_{min}$  characterises the minimum retinal spot size that can be obtained, i.e. even if the source (the ‘object’ that emits the radiation in the optical sense and is imaged onto the retina) would itself be characterised by an angular subtense of less than  $\alpha_{min}$ . Currently  $\alpha_{min}$  has the numerical value of 1.5 mrad, i.e.  $\alpha_{min} = 1.5\ mrad$  which in a human eye with an ‘air-length’ of 17 mm is equivalent to a retinal spot diameter of 25.5  $\mu m$ . There is also a ‘*maximum angular subtense*’ with the symbol  $\alpha_{max}$  and the current numerical value of 100 mrad, i.e.  $\alpha_{max} = 100\ mrad$ . In contrast to  $\alpha_{min}$ , the maximum angular subtense of 100 mrad (equivalent to angle in degrees of  $5.7^\circ$  and to a diameter of 1.7 mm at the retina in the human eye) does not reflect an actual optical limitation of the retinal image size, but rather characterises a breakpoint in the dependence of the retinal thermal hazard on the diameter of the retinal spot size, as will be discussed further below.

The retinal thermal MPE values depend on the angular subtense of the apparent source by way of the factor  $C_6$  (or  $C_E$  in ANSI and ICNIRP documents), which is defined as

$$C_6 = \frac{\alpha}{\alpha_{min}} = \frac{\alpha}{1.5\ mrad}$$

where  $\alpha$  is given in units of mrad and is limited to values between  $\alpha_{min}$  and  $\alpha_{max}$ . If the actual angular subtense of the apparent source is less than 1.5 mrad, the value of 1.5 mrad is assigned to  $\alpha$ ; if it is larger than 100 mrad, the value of 100 mrad is assigned to  $\alpha$ . For sources larger than 100 mrad it is important to note that the angle of acceptance for determination of the exposure level that has to be compared to the MPE value must also be limited to 100 mrad for this

---

<sup>2</sup> The challenge to define a ‘thermal diameter’ for an arbitrary retinal irradiance profile is discussed elsewhere [6, 7, 8], here we concentrate on the general dependence of the damage threshold on varying retinal spot sizes where usually the profile is a top hat unless noted.

analysis to be correct. It is pointed out that the specification of  $C_E$  in the ICNIRP guidelines and in Table 6 of the current version of the ANSI laser safety standard can be misinterpreted to mean that  $\alpha$  is not limited to 100 mrad and  $C_E$  can increase beyond 66.6, even though the measurement angle of acceptance (also referred to as limiting cone angle) is limited to 100 mrad. This, however, would grossly underestimate the hazard. Limiting the angle of acceptance to 100 mrad and limiting  $\alpha$  to  $\alpha_{max} = 100$  mrad, is equivalent to increasing  $C_6$  beyond 66.6 with  $\alpha^2$  only when an open field of view for the determination of the exposure level is used. This  $C_6$  for  $\alpha > 100$  mrad and open measurement field of view should ideally also have a different symbol (here  $C_6^{open}$  is used) and can be derived in the following way [6].

$$C_6^{open} = 66.6 \frac{\alpha^2}{\alpha_{max}^2} = \frac{\alpha_{max}}{\alpha_{min}} \frac{\alpha^2}{\alpha_{max}^2} = \frac{\alpha^2}{\alpha_{min} \alpha_{max}}$$

That is, when the MPE is determined with  $C_6^{open}$ , the angle of acceptance of the measurement shall not limit the exposure assessment and the total energy that passes through the 7 mm aperture is relevant in the comparison with the MPE, which makes it the superior representation in the discussion of the spot size dependence in this paper and for the comparison to experimental threshold values which are given in terms of TIE (i.e. not limited by an angle of acceptance of  $\gamma = 100$  mrad). However, it has to be noted that when the retinal irradiance profile is not a top hat and features some regions with higher local irradiance, then it is not appropriate to use an open field of view, rather, the source needs to be scanned for the maximum value with a given field of view equal to  $\alpha_{max}$  (i.e., currently 100 mrad).

The general dependency of the exposure limits when expressed in terms of corneal space (i.e. the usual MPE representation) and in terms of retinal radiant exposure are shown in figure 1a and 1b, respectively (values for pulse durations between 1 ns and 18  $\mu$ s for visible radiation).

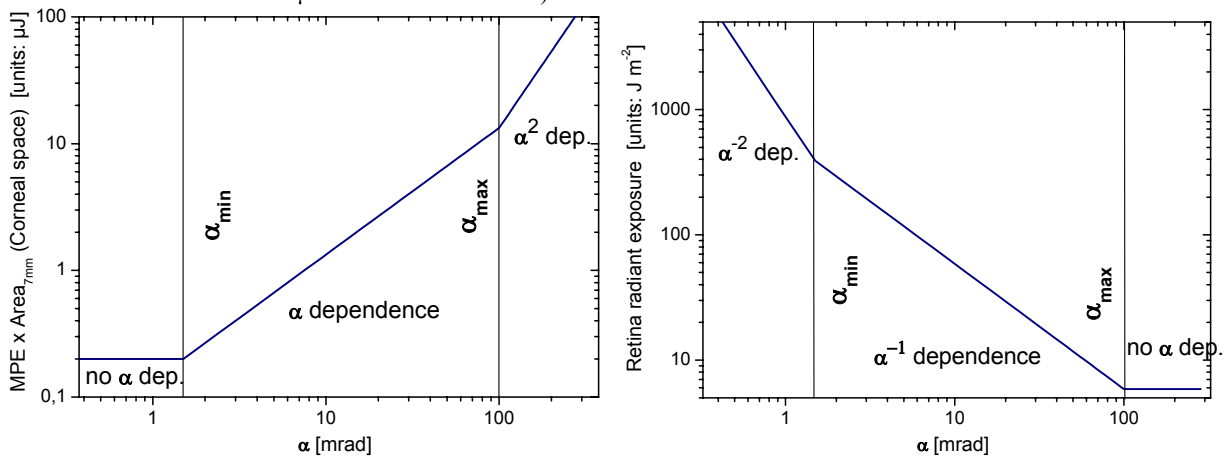


**Fig. 1** *Left:* General dependence of the current MPE values (which are specified as corneal levels) as function of  $\alpha$ . *Right:* General dependence of the current MPE values when specified as retinal radiant exposure as function of  $\alpha$ , assuming an ocular transmittance of 1.

Retinal damage threshold values also can be presented in two equivalent ways, either in terms of TIE in units of Joule, or in terms of retinal radiant exposure in units of  $J m^{-2}$ . To facilitate the comparison between different models and the human case, the spot size is given in terms of diameter ( $\mu$ m) and not in terms of angular subtense, since the diameter is the basic quantity and the angular subtense depends on the length of the eye, which is different for the rhesus monkey and the human (i.e. for the same angular subtense, the image on a rhesus monkey retina is smaller than on a human retina).

### 1.3 Current status

The current retinal spot size dependence of the MPEs, in principle, reflects that a larger spot, for the same retinal radiant exposure, produces a higher temperature rise than compared to a smaller spot where radial heat flow reduces the temperature in the centre of the spot. Without radial cooling playing a role, the damage threshold in terms of retinal space (retinal radiant exposure) would not depend on the diameter of retinal spot and in terms of corneal space the MPE would depend on  $\alpha^2$ . Due to decreased radial cooling for larger retinal spots, this  $\alpha^2$  increase with retinal spot size is

decreased to a dependence of ‘only’  $\alpha$ . When the spot size becomes so large that the effect of radial cooling does not reach the centre of the spot, the temperature in the centre of the spot is determined by the local radiant exposure only, independent of the retinal spot size. It follows that the damage threshold in terms of retinal radiant exposure does no longer depend on the spot diameter, which is the physical background of the spot size dependence breakpoint, i.e. of  $\alpha_{\max}$ . The value of  $\alpha_{\max} = 100$  mrad and a linear dependence of  $\alpha$  up to  $\alpha_{\max} = 100$  mrad of the current MPEs is based on very limited and early experimental spot size dependence threshold studies, the basic one was conducted with a rabbit model [9]. The current spot size dependence of the MPEs, however, is under doubt for some time, especially for pulse durations in the microsecond range and for shorter pulses, since in the condition of thermal confinement (i.e. when the pulse duration is shorter than the time it takes for heat flow to have an effect) it would not be expected that the threshold in terms of retinal radiant exposure would depend on the diameter of the retinal spot, but should depend only on the local radiant exposure value. This concern was also supported by a spot size dependence study published in 2000 [10] for nanosecond and microsecond pulse durations. These experimental thresholds (figure 2) exhibit an  $\alpha^2$  dependence for spot sizes above 80  $\mu\text{m}$  for the 5 ns data and above about 200  $\mu\text{m}$  for the 3  $\mu\text{s}$  data, as would also be predicted by thermal models.

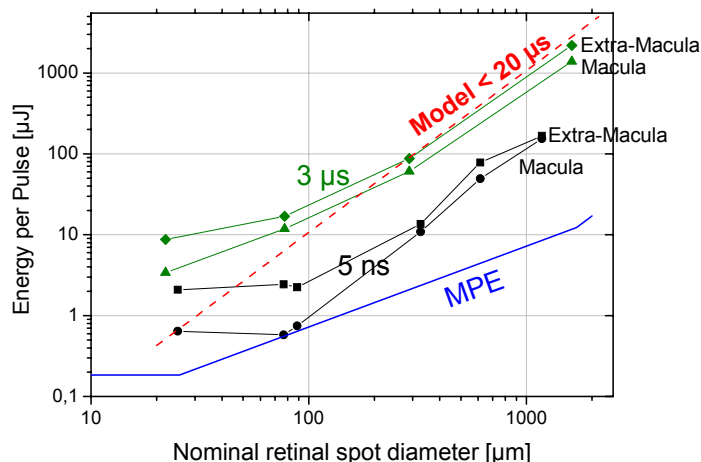


**Figure 2.** Experimental 24h threshold values for 3  $\mu\text{s}$  (590 nm) and 5 ns pulses (532 nm) from Zuclich et al. [10].

However, the thresholds for spot sizes smaller than these breakpoints do not follow this expected  $\alpha^2$  dependence and this “small spot – spot size behaviour” presents an even bigger challenge for interpretation and understanding. Till et al. [11] proposed a new damage model (different from the traditional Arrhenius damage integral) that fits this microsecond small spot data. However, similar small spot threshold behaviour is also found for millisecond as well as ultrashort pulse durations [12]. In this paper, we propose a generic explanation of the small spot size dependence, which can explain experimental in vivo threshold values for all pulse duration. The discussion is also very relevant for the problem that the 5 ns pulse duration 77  $\mu\text{m}$  retinal spot diameter threshold is basically at the current MPE value (figure 2), i.e. there is a need that the MPEs are reduced. Our discussion of the transition from thermally based damage thresholds to the regime of thresholds based on bubble formation around melanosomes is also relevant in this respect.

## 2. MATERIALS AND METHODS

### 2.1 Experimental setup

Figure 3 shows a schematic overview of the setup for the irradiation of the samples. Two frequency-doubled Nd:YAG lasers (Omicron FK-LA 8000) provide continuous laser radiation at a wavelength of 532 nm and with a total output power of up to 18 W. These lasers have a beam propagation factor  $M^2$  of about 8. To achieve small spots (23  $\mu\text{m}$ ), a continuous frequency-doubled Nd:YAG TEM<sub>00</sub> laser (CrystaLaser GCL-100-L) with a wavelength of 532 nm and 100 mW output power was used to produce a Gaussian spatial distribution on the sample.

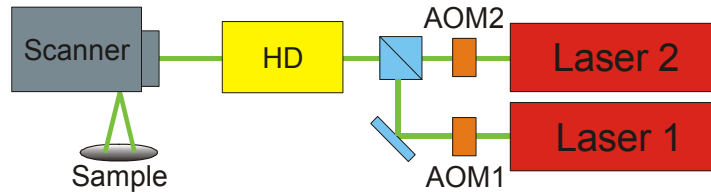


**Figure 3.** Experimental set up for the *in vitro* exposures.

In front of each laser aperture, a computer controlled acousto-optical modulator (AOM1 and AOM2) was placed. With the AOMs it is possible to adjust the transmitted power in 1024 steps between “fully open” and “zero transmission” with high temporal resolution. Thus the AOMs control both the pulse duration (with arbitrary pulse shapes being possible), as well as the peak power for each pulse. After combining the two laser beams by a polarization crystal, the beam undergoes a homogenization process (denoted by a homogenization device HD in figure 3) to achieve a circular top hat spatial beam profile at the sample. This was done by coupling the beam into a 200  $\mu\text{m}$  fiber and imaging its tip by focusing lenses. The beam profile for a spot diameter of 120  $\mu\text{m}$ , 549  $\mu\text{m}$  and 2000  $\mu\text{m}$ , respectively, is shown in Figure 4. The beam finally enters a galvanometer-driven scan head (SCANLAB hurrySCAN™ 14) which produces a computer controlled scan pattern on the sample.

Concurrent control of the scanner and the AOMs was affected with a PC interface card (SCANLAB RTC® 4) and a self-developed computer program. With this computer program it is possible to expose a sample with a grid of individual laser exposures in a short amount of time. For instance, for small laser spots (23  $\mu\text{m}$ ) it is possible to place 200 exposures with varying energy per pulse on a sample area of 5 x 5  $\text{mm}^2$  within one minute.

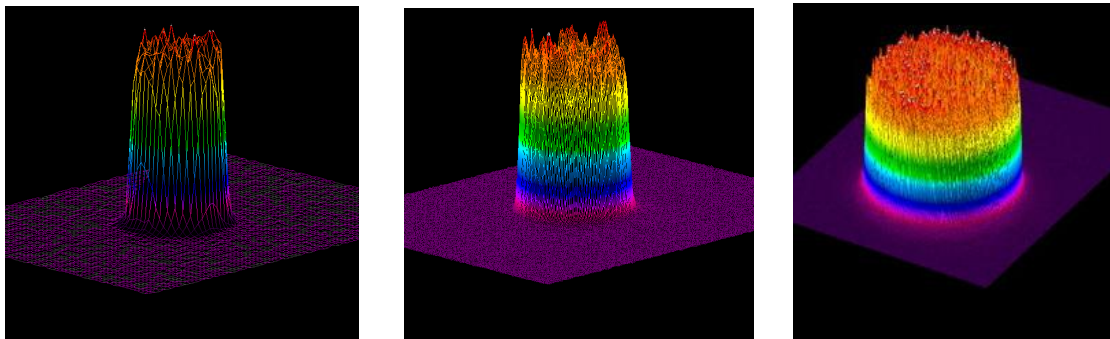


**Figure 4.** Beam profiles for spot diameters of 120  $\mu\text{m}$ , 549  $\mu\text{m}$  and 2000  $\mu\text{m}$ , respectively, from left to right.

Prior to the exposures, the spatial beam profile was recorded in the sample plane with a COHU CCD-camera (model 7512) with 6.7  $\mu\text{m}$  pixel pitch (figure 4), and the beam diameter defined at the 1/e level was calculated with beam analyzer software (Spiricon LBA-700PC). Furthermore, a calibrated power detector (Ophir 3A and Ophir L40(150)A, respectively) was placed beneath the scanner before and immediately after the exposures to record the power incident on the sample for an “open” AOM, i.e. the maximum peak power level. The actual energy deposited on each irradiated location on the sample was calculated in Microsoft Excel, using pulse length, power, and the AOM’s throughput setting.

## 2.2 Sample preparation and analysis

The *in vitro* explant samples were obtained from fresh bovine eyes which were received from a local slaughterhouse. After dissection of the surrounding connective tissue, the eye was opened approximately 7 mm beneath its equator and the vitreous body was removed. The black-pigmented parts of the fundus of the eye were cut into rectangular pieces and placed in phosphate-buffered solution. The sensory retina (the photoreceptor layer and attached nerve layers) was gently peeled-off approximately five minutes afterwards so that the uppermost layer was the retinal pigment epithelium (RPE), supported by the choroid and the sclera. Then, the tissue was stained with the viability marker Calcein AM (2.5  $\mu\text{M}/\text{ml}$  phosphate buffered saline). Calcein is absorbed by the vital cells and reduced to a fluorescent dye by means of cellular esterases (excitation maximum at 490 nm, emission at 520 nm). After 30 minutes incubation time, the sample was put into a specially designed sample holder and examined with a microscope. Following the laser exposure of the samples, the examination was done with a Zeiss Axiovert inverted microscope. The examination took place between 15 min and

1 hour after exposure. Vital cells show a bright green fluorescence, whereas the damaged cells appear dark due to loss of dye. The examination was performed by one of us only (JH) due to time constraints regarding the viability of the samples. A horizontal and vertical line with overexposed “shots” formed a cross in the exposure grid to aid the evaluation. Exposed sites were determined to be either “damaged”, or “not affected”. It was noted that on occasions, the exposed area appeared distinctively brighter than the surrounding non-exposed area or that highly fluorescent droplets formed at the edge of the region where cells were dark. For very small laser spots, it occurred that only droplets could be seen and it was not possible to determine whether the cell “behind” the droplet appeared dark (i.e. dead) or fluorescent. The exact reason for this increased brightness and formation of droplets is not known but is expected to be related to leaking of Calcein out of compromised cells. These cases were also counted as “damaged”. The lesion dose-response data was evaluated by a Probit analysis software (ProbitFit V1.0.2 by Brian Lund, Northrop Grumman) to obtain ED50 and slope values [5]. The finite difference thermal damage model is to be described elsewhere [13].

### 3. RESULTS

#### 3.1 *In vitro* bovine and computer model

*In vitro* damage thresholds (ED50) of bovine retinas are shown in figure 4, together with results of the finite difference computer model. The computer model data was obtained assuming a minimal visible lesion with a diameter of 20  $\mu\text{m}$ . Data are provided for the pulse duration range of 1 ms to 655 ms and a spot size diameter range of 23  $\mu\text{m}$  to 2 mm. The slope  $S$  (ED84/ED50) of the ex-plant *in vitro* thresholds is close to 1 (typically around 1.1, but never larger than 1.4), indicating both little variability within different eyes as well as a small uncertainty [5].

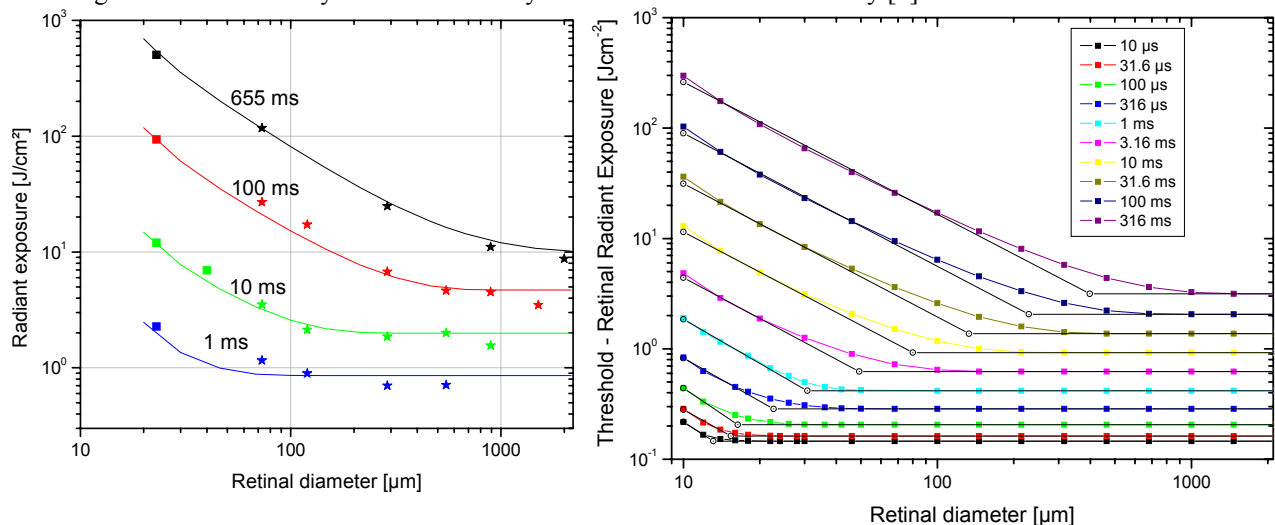


**Figure 5. Left:** Damage threshold values for bovine *in vitro* samples plotted as retinal radial exposure. Square symbols indicate a Gaussian beam profiles (small spots), star symbols represent top-hat profiles. The full lines are the result of a finite difference computer model assuming a top hat profile, described in [13]. **Right:** Computer model threshold data with tighter spacing of data and larger ranges than the current threshold data.

The computer model indicates that the difference in threshold between a top hat profile and a Gaussian profile is about 1.2 for small spots, which also is approximately shown by *in vitro* exposures with Gaussian beam profiles with larger diameters (not shown here.) The analysis of different beam profiles and an appropriate diameter definition is ongoing work and will be reported at BIOS 2007.

Two regions can be clearly distinguished in figure 5, one where the logarithmic slopes of the curves (threshold as function of diameter  $d$ ) are close to -1, i.e. an approximate  $1/d$  dependence, and another where the thresholds do not depend on the diameter  $d$ , i.e. a logarithmic slope of 0. These two regions are separated by a ‘knee’ in the curve, which can be approximated by a breakpoint when straight lines (in logarithmic coordinates) are fitted to the left and to the right part of the curves. The position of the breakpoint depends on the pulse duration: for pulse durations less than 20  $\mu\text{s}$ , there is no breakpoint discernible in the computer model data and the thresholds in terms of radiant exposure all have the same value irrespective of the spot diameter, while for long exposure durations, a breakpoint can be identified that

shifts in position depending on the pulse duration. As the knee is moving out of the modeling range for pulse durations less than about 20  $\mu\text{s}$ , the threshold data for these and smaller pulse duration exhibit no spot size dependence, but a constant retinal exposure threshold value.

The threshold data can also be plotted as function of pulse duration for a given spot size (figure 6). The dependence of the threshold as function of pulse duration for pulse durations longer than approximately 1 ms can be fitted well with a straight line in log-space and equals  $t^{0.9}$  for small spots and  $t^{0.41}$  for large spots.

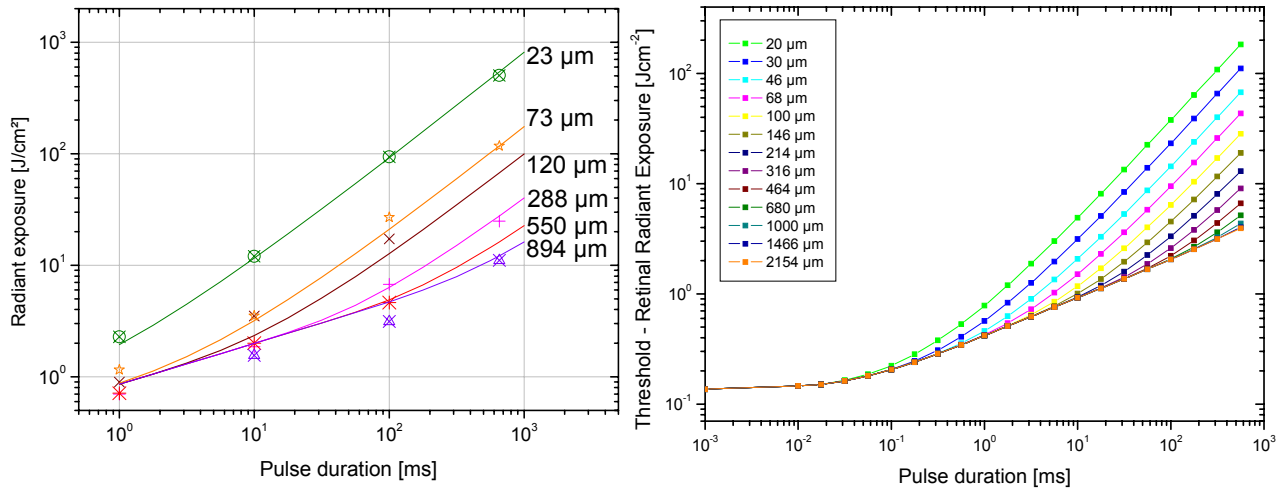


**Figure 6** Threshold data plotted as function of pulse duration for a range of retinal spot size diameters. Left: *in vitro* threshold data and computer model. Right: computer model threshold data.

### 3.2 New 100 ms monkey threshold data

Recently, a series of Rhesus monkey thresholds were determined with a 514 nm Argon laser and a pulse duration of 100 ms with varying retinal spot diameters [14] as shown in figure 7. The profile was Gaussian for the smaller spots and top hat for the larger spots. In figure 7, the diameter is not the actual diameter at the monkey retina (which is not known) but rather a nominal value which would apply for a perfect optical system. The value of the nominal retinal laser spot diameter is derived from the measured far field divergence of the laser beam which is equal to the angular subtense of the retinal image for an eye which is accommodated to infinity. This nominal value is to be differentiated from the actual retinal spot diameter which might be larger due to, for instance, scattering. The laser beam diameter at the cornea was 2.5 - 3 mm to minimize the influence of aberrations of the eye.

The rhesus monkey data (1 hour and 24 hour endpoint, macula and extramacula) are shown in figure 7 together with damage threshold data of the bovine *in vitro* model as well as the finite difference computer model. The monkey 514 nm 100 ms data is compared with the *in vitro* bovine threshold data (532 nm) for retinal spot diameters between 136  $\mu\text{m}$  and 562  $\mu\text{m}$  in table 1.

**Table 1.** New 100 ms Rhesus monkey thresholds (determined 24 h after exposure) and *in vitro* bovine (explant) thresholds

Diameter $\mu\text{m}$	Monkey		Explant	Factor
	Macula mJ	Extramacula mJ	mJ	
136	1,8	1,7	1,9	1,1
281	3,6	4,0	4,5	1,3
562	8,6	9,4	11,0	1,3

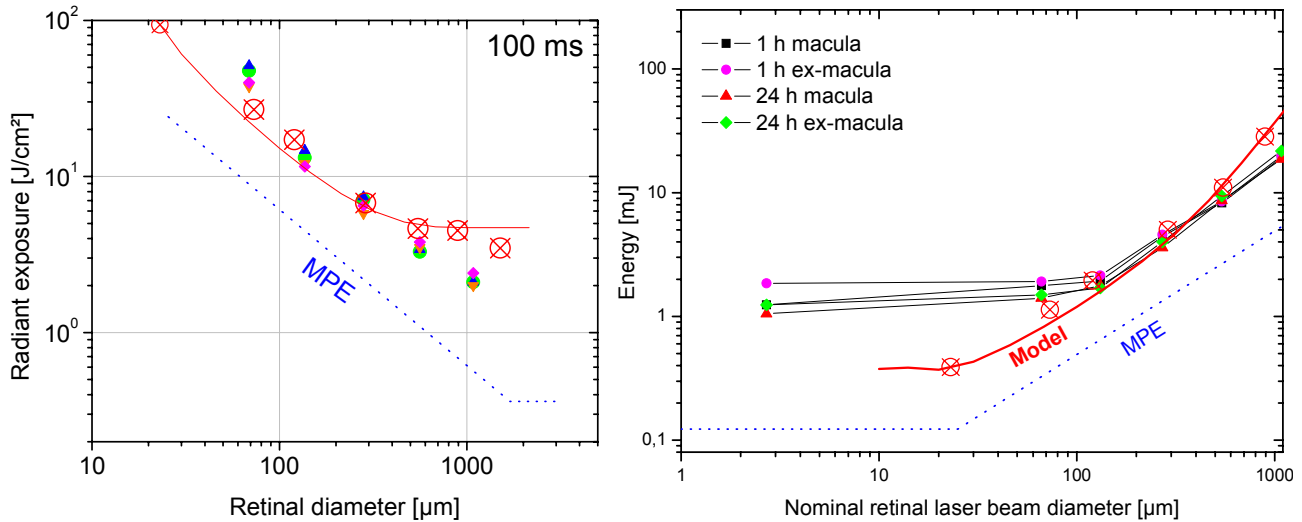


**Figure 7.** Rhesus monkey threshold data (coloured small symbols), bovine *in vitro* threshold data (large red crossed circles), model data (full red line) and the current MPE values (blue dotted line). The data is plotted as retinal radiant exposure (not corrected for transmission losses for the case of Rhesus monkey) on the left and in terms of IOE on the right ('corneal space').

### 3.3 Other threshold data

In published laser threshold studies, no monkey threshold data are available where the spot size dependence in terms of the breakpoint between  $1/d$  threshold dependence and no spot size dependence for the retinal radiant exposure can be evaluated, because the retinal spot sizes do not reach to large enough diameters. However, data is available for the  $1/d$  threshold dependence region [15, 16] for pulse durations of 250 ms and 1 s. Threshold data is published also for short pulses and these exhibit no spot size dependence when plotted as retinal radiant exposure, including 2 ms pulse duration data [17] as well as microsecond and nanosecond data [10]. The only monkey retinal threshold data which covers a large enough spot size range in the millisecond range to is for Xenon arc lamp exposure [17], and these data do very clearly show the predicted breakpoint with  $1/d$  dependence to the left of the breakpoint and no spot size dependence of the retinal radiant exposure thresholds for spot sizes larger than the breakpoint. For both the Beatrice et al. (514 nm, 1 s pulse duration, 1 h endpoint) [15] and the Allen et al. (694 nm 2 ms pulse duration, 5 min endpoint) [17] laser data, the thermal computer model and the *in vitro* bovine threshold predict the NHP thresholds to within 30%. In respect to the Ham et al. data (633 nm, 250 ms and 1 s, 24 hour endpoint) [16], and the Allen Xenon lamp data (4 ms to 100 ms pulse duration, 5 min endpoint) [17] the computer model and *in vitro* model thresholds are a factor of between 2 and 3 lower than the monkey data. However, the relative spot size dependence, including a breakpoint in the 100 ms Xenon lamp data is predicted very well. An analysis of all the available Rhesus monkey laser thresholds for pulse durations between 1 ms and 1 s shows, that the experimental uncertainty from one set of experimental data is also in some cases within a factor of 2.

## 4 DISCUSSION

### 4.1 Comparison with monkey 100 ms data

The data given in Table 1 show that for retinal spot sizes larger than about 100 μm, the *in vitro* bovine thresholds agree to within a factor of 1.3 with the 24 h Rhesus monkey threshold data (the small spot data is discussed in the following subsection). It is noted that Rhesus monkey 1 h and 24 h threshold data as well as the extra-macula and macula thresholds are also very similar with each other and only differ noticeably (in the typical way, i.e. macula lower than extra-macula and 24 h thresholds lower than 1 h [5]) for spot sizes less than 100 μm. The monkey threshold for a diameter of 1080 μm is lower than the interpolated *in vitro* bovine threshold. The reason for this difference is not entirely clear but could be due to the non-perfect top hat profile of the monkey threshold. An inner region of higher retinal irradiance could lead to a smaller effective thermal diameter, so that this threshold in terms of TIE would have to be plotted at a smaller nominal retinal diameter – for instance, if this effective thermal diameter were 750 μm, it would lie on the curve

predicted by the computer and bovine model. The spot size dependence in the spot diameter range between 100  $\mu\text{m}$  and 500  $\mu\text{m}$  when plotted as retinal radiant exposure is almost exactly  $1/d$ , i.e. the logarithmical slope of the threshold curve is, within the experimental uncertainty, identical to  $-1$ . Unfortunately, the monkey data currently does not include large enough spot sizes to reach up to the breakpoint as seen in the *in vitro* bovine and computer models.

The closeness of the thresholds for the different models<sup>3</sup> for spot sizes larger than 100  $\mu\text{m}$  might be surprising due to the difference of the *in vivo* monkey and the *in vitro* bovine models and endpoints. For the *in vitro* bovine samples, the RPE cell layer is exposed directly, i.e. there is no optical loss (reflection or absorption) due to pre-retinal media as in the monkey eye, as well as there is no pre-RPE influence on the laser profile (such as scattering). The transmittance associated to the rhesus monkey pre-retinal media equals 0.57 [18], the inverse of 0.57 equals 1.7 and by this factor, the monkey TIE threshold should be higher. However, the *in vitro* bovine sample is at room temperature (about 22  $^{\circ}\text{C}$ ) and the monkey body temperature is about 38  $^{\circ}\text{C}$ , resulting in a lower threshold for the monkey. The computer model predicts a difference in thresholds by a factor of 1.5 for these two different background temperatures, compensating to a large degree for the difference in optical transmissivity.

More importantly for the validation of the *in vitro* bovine model are the different endpoints. The *in vitro* bovine thresholds are determined at about 5-15 minutes after exposure and they are based on RPE cell viability. Monkey thresholds on the other hand are determined ophthalmoscopically (i.e. optical appearance change) 1 h and 24 h after exposure. From the similarity of the threshold data for spot sizes larger than 100  $\mu\text{m}$  it appears that the underlying mechanism is in both cases immediate RPE cell damage even though the endpoints are different. For the case of the monkey threshold experiments, the viability of RPE cells can not be determined and detection of a lesion is based on a change of visual appearance, i.e. change of colour or reflectance of the retina, where the uppermost layer that is imaged is the sensory retina, not the RPE (outside of the fovea, the sensory retina has a thickness of about 200 to 300  $\mu\text{m}$ ). It appears that the change of appearance of the sensory retina for the monkey 1 h and 24 h thresholds is caused by the physiological reaction of the system to the dead RPE cells. This reaction takes some time to develop, and after that time becomes noticeable as a visible change of appearance. It is important to distinguish these changes of retinal appearance at threshold levels determined 1 h and 24 h from superthreshold injuries and from threshold levels necessary to induce an immediately visible lesion, such as in medical photocoagulation. In the latter cases, the induced effect is coagulation of the RPE and the sensory retina, which requires higher temperatures and higher retinal radiant exposures than 1 h and 24 h thresholds, which are the more appropriate endpoints for setting safety exposure limits.

#### 4.2 Small spot – spot size behaviour

In the previous subsection we have concluded that the underlying damage mechanism for both the *in vivo* Rhesus monkey 1 h and 24 h ophthalmoscopically visible thresholds as well as the *in vitro* bovine model is likely to be immediate thermal damage of RPE cells. For spot sizes above 100  $\mu\text{m}$ , both models yield almost identical threshold levels. However, for spot diameters less than 100  $\mu\text{m}$ , there is striking deviation of both the computer model and the *in vitro* bovine model thresholds from the monkey thresholds. In terms of TIE (total energy incident on the retina), the monkey thresholds remain almost constant for smaller laser spots, while both the *in vitro* bovine as well as the computer model continue to decrease with basically a linear spot diameter dependence. At a nominal laser spot diameter of 25  $\mu\text{m}$ , the *in vitro* bovine and the computer model thresholds are a factor of about 3.5 lower than the interpolated monkey threshold. Very similar small spot - spot size behaviour is also noted for 532 nm nanosecond thresholds [10] (figure 2). As shown in [12], equivalent small spot – spot size dependence can also be observed for millisecond pulses and ultrashort pulses. Till et al. developed a special “slow damage” model based on melanosome membrane melting [11] to explain the microsecond small spot data, which could, however, not be applied to explain the nanosecond small spot behaviour. The existence of this ‘peculiar’ small spot behaviour for pulse durations that clearly encompass different damage mechanisms (for instance also including bubble formation around melanosomes, see discussion in subsection 4.5) indicates that the underlying effect is more generic or basic and does not depend on the damage mechanism. Two explanations can be envisaged:

- 1) the laser spot that is incident on the RPE is enlarged up to about 80  $\mu\text{m}$  - 100  $\mu\text{m}$  diameter even if the nominal laser spot diameter is smaller than that
- 2) the laser beam at the retina and RPE is not enlarged but there are factors for the monkey experiments which are related to the non-visibility of small lesions at lower thresholds. The lower bovine and computer model

---

<sup>3</sup> All three, Rhesus monkey, *in vitro* bovine and computer program are, after all, intended as a model for human damage thresholds

thresholds indicate that also in the monkey retina (if the retinal spot at the RPE is not enlarged), RPE cells would be damaged at levels lower than those determined experimentally and shown in figure 7. In that case, at the threshold levels determined by the bovine and computer model, also the monkey RPE cells would be damaged, and the diameter of the damaged region RPE is not larger than the nominal laser beam diameter. The observed monkey thresholds can be explained when, for some reason, these small diameter RPE lesions in the monkey eye do not produce the necessary change of optical appearance that is necessary to be detected as ophthalmoscopically visible lesion. This could be due to two reasons.

- i) A small diameter RPE lesion does not invoke the systemic response that leads to a change of optical appearance of the sensory retina (i.e. an RPE damage is present, but the systemic response seen for larger RPE lesions does not occur). If this explanation were true, the question would remain if this would be a significant lesion in terms of having an effect on vision or not. There are reports that single dead RPE cells do not lead to damage of the associated photoreceptors but are replaced by neighbouring RPE cells sliding into place [19]. This effect is for instance to be exploited for a novel therapeutic technique.
- ii) An optical change of the sensory retina is only noticeable when it has a minimum diameter, i.e. small RPE lesions might induce small diameter systemic responses in the sensory retina, but they are too small to be detected ophthalmoscopically, for instance due to lack of contrast.

In both cases, i) and ii), the laser energy per pulse needs to be correspondingly higher to produce a “superthreshold” RPE lesion, i.e. an RPE lesion with a diameter larger than the actual laser beam profile incident on the RPE, which then forms a change of appearance of the retina that is detectable ophthalmoscopically. The computer model can be used to model this case, when the minimum lesion diameter of the model is set equal to 100  $\mu\text{m}$  for the case that the laser beam has a diameter of less than 100  $\mu\text{m}$ . In this case, for a pulse duration of 100 ms, the computer model thresholds exactly match the monkey thresholds. However, this explanation number 2) can still be ruled out, since for pulse durations of 1 ms and below, the energy per pulse necessary to create a lesion significantly larger than the laser beam (for the case that the laser beam diameter is less than 100  $\mu\text{m}$ ) would be a factor of at least three larger than the threshold for a 100  $\mu\text{m}$  spot, which is not observed experimentally (the threshold for smaller nominal laser spots remains constant or decreases to some extent, when compared to the threshold for 80  $\mu\text{m}$  to 100  $\mu\text{m}$  spot diameters). Also the calculated temperatures in the center of the laser spot would reach unrealistic values, for instance for a 25  $\mu\text{m}$  laser spot and a pulse duration of 1 ms almost 4000  $^{\circ}\text{C}$ . Also, this spot size behaviour is seen for 5 ns pulse durations [10] where the damage mechanism at threshold appears to be bubble formation around the melanosomes in the RPE (see following subsection) and for this damage mechanism, which relies on rapid heating in the thermal confinement regime, it is physically impossible to create the temperature rise necessary for bubble induction in an RPE region significantly larger than the actual region that is exposed to laser radiation and at the same time exhibit thresholds that are not higher than the threshold where the laser spot is actually 80  $\mu\text{m}$ .

Ruling out explanation number 2 leaves explanation number 1; an increase of the laser beam diameter on its path to the RPE. The obvious reason for an increase of the laser beam profile is either scattering or aberration, i.e. wavefront distortion. Aberration is small for small laser beam diameters at the cornea, which leaves scattering as main explanation. Forward scattering in the pre-retinal media, after all, is given as the reason for the current  $\alpha_{\text{min}}$ , which is equivalent to a retinal image diameter of 25  $\mu\text{m}$  [20] while the diffraction limited laser spot diameter for a perfect optical system would rather be in the range of 6  $\mu\text{m}$ . However, it seems unlikely that pre-retinal scatter can induce an increase of the retinal image of up to 100  $\mu\text{m}$ , since it would severely hamper vision, which is not the experience we have as humans (it can be assumed that the monkey visual acuity is comparable). Rather than pre-retinal scattering, we would like to offer a new explanation of the small spot - spot size behaviour in the visible wavelength range, namely intra-retinal scatter. This explanation is substantiated by backscatter images obtained in optical coherence tomography (OCT) where the backscatter signal of the uppermost layer of the sensory retina, the nerve fibre layer (NFL), is relatively strong, even for the usual OCT wavelength of 800 nm (figure 8). It appears reasonable that a laser beam with a diameter of for instance 25  $\mu\text{m}$  at the NFL can be increased to a diameter of about 80  $\mu\text{m}$  to 100  $\mu\text{m}$  at the RPE, with a distance between the NFL and the RPE of approximately 200  $\mu\text{m}$  – 300  $\mu\text{m}$ .

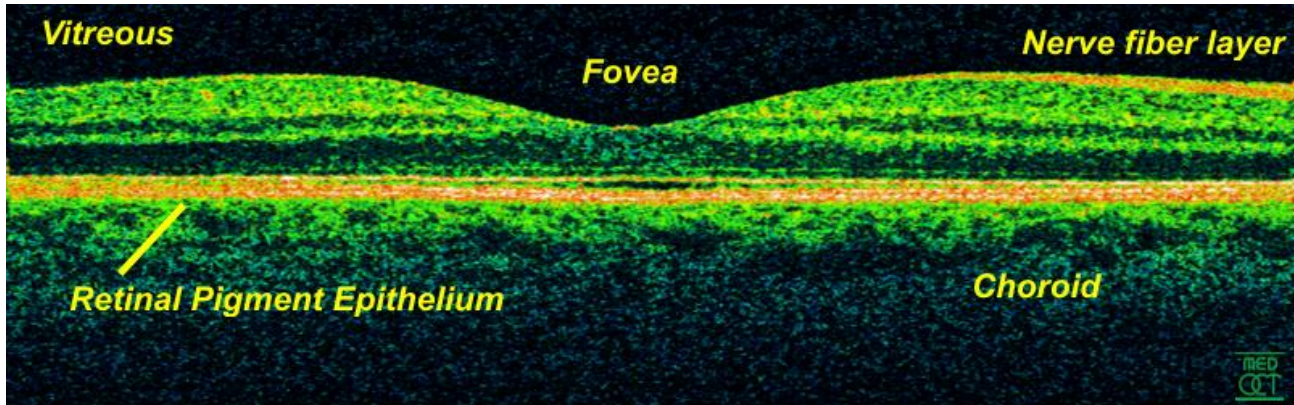


**Figure 8.** OCT image of human retina. The nerve fiber layer is shown as relatively strong backscatterer with red pixels. In the center, the foveal pit. Source: Department of Medical Physics, Medical University Vienna, Austria (GNU Free Documentation Licence).

Povazay et al. [21] compared a number of wavelengths and noted that no backscatter signal from the RPE could be detected for blue 475 nm wavelength, and only a very weak signal for the red 605 nm wavelength. At the usual wavelength of 800 nm, OCT images still show a relatively strong backscattered signal from the NFL. For setting exposure limits, however, it is important to note that the NFL is pushed aside in the foveal pit to increase visual acuity there. The OCT backscatter signal from the sensory retina is minimal in the foveal region (see figure 8) which also ties together with our experience that we have high visual acuity in the fovea only and low acuity vision outside of the foveal region. Therefore it is to be expected that in the foveal region, a minimal laser beam (25  $\mu\text{m}$  diameter for instance) is not significantly increased in diameter due to scattering, i.e. it might well be that for direct exposure of the fovea, the damage thresholds are lower than the ones determined experimentally for the Rhesus monkey outside of the fovea. The question remains if these foveal lesions of the order of about three RPE cells or less have an effect on vision. After all, the thresholds predicted by *in vitro* bovine and computer models for minimal 25  $\mu\text{m}$  diameter laser spots for 100 ms pulse durations are only a factor of 3 above the current MPE, which is also the case for longer exposure durations, i.e. for 250 ms. Assuming that damage of the RPE is the basic damage mechanism for both thermally induced lesions and bubble formation at threshold levels, then the bovine and computer model thresholds indicate that for exposure levels not more than three times above the MPE, damage of RPE cells should occur in the monkey RPE. This damage would also occur in the human eye, when the absorption properties of the retinas are comparable. Unfortunately, threshold studies for humans are rare, but those available indicate that the thresholds for Caucasians are a factor of about two higher than those for the Rhesus monkey (see references in [5]), which is believed to be due to differences in pigment density. However, pigment density in the retina are higher in Negroid human retinas than in Caucasian retinas, and the difference in pigmentation might also be significant only regarding pigmentation of the choroid, since it appears that the pigment density in the RPE is similar in most vertebrates. In that respect it is important to note that the damage thresholds only depend on choroidal pigment density for exposure durations in the hundreds of millisecond range and longer. For exposure durations in the millisecond range and shorter, the threshold is mainly determined by the amount of energy absorbed in the RPE (see [13]). This needs to be further discussed in the committees setting the laser exposure limits as well as in relation to the risk associated with the use of Class 3R (or according to CDRH [22] Class IIIa) lasers, which feature emission levels of up to a factor of five times above the MPE.

#### 4.3 General spot size dependence

As shown in figure 5, the finite difference thermal model can predict *in vitro* bovine thresholds for 532 nm laser exposure, within the covered pulse duration range of 1 ms to 655 ms and retinal spot sizes between 23  $\mu\text{m}$  and 2 mm very well. Both models, *in vitro* bovine and computer model, agree very well with 514 nm Rhesus monkey threshold spot size dependence data for 1 s exposure duration [15] as well as new 100 ms pulse duration data [14]. The two available rhesus monkey data sets for the red wavelength range [16, 17] differ by at least a factor of two when compared to each other. However, the relative retinal spot size behaviour of these data sets is predicted well by the *in vitro* bovine and the computer model, which is also the case for monkey Xenon lamp threshold data [17]. It can be concluded that the thermal damage computer model and the *in vitro* bovine model, for pulse durations between 1 ms and 1 s, for all

retinal spot sizes, can be a valuable tool for the absolute prediction of non-human primate and human threshold levels, for instance for arbitrary retinal laser profiles or for scanned laser radiation.

The thermal model and the *in vitro* bovine threshold data show a previously unknown variation of the spot size dependence for different pulse duration. When expressed as retinal radiant exposure values, the breakpoint between the 1/d threshold dependence and the constant threshold region for larger spots is not constant, as currently implied by the MPEs, but shifts to smaller diameters for shorter pulses. The breakpoint is in the region of 100 mrad (1.7 mm) only for pulse durations longer than 1 s. For pulse durations of less than approximately 100  $\mu$ s, there is no detectable spot size dependence, i.e. the damage threshold is a constant retinal radiant exposure value, independent of the actual laser spot size. This apparent dependence of the breakpoint can also be explained based on thermal diffusion. The thermal diffusivity is a characteristic parameter that can be understood as the speed by which heat diffuses through a medium, or by which a temperature difference travels. The thermal diffusivity  $D_{th}$  is defined as the ratio of thermal conductivity over the specific heat and the density of the material and thus has the units of  $cm^2/s$ . Within a time  $t$ , a 'heat wave' travels approximately a distance of about  $2\sqrt{t D_{th}}$ . This 'speed' is also relevant for the radial cooling of the laser spot. As the heat wave travels into radial direction away from the rim of the disk that is heated by the laser spot, it heats the surrounding non-irradiated region. Due to this heat flow, the irradiated area is cooled, so that the zone that is affected by this cooling action (a 'negative heat wave', i.e. a cooling wave) travels inwards from the rim of the laser spot, towards the centre of the laser spot. As long as the 'cooling front' does not reach the centre of the laser beam, the temperature of the centre of laser spot remains unaffected from the radial cooling action, i.e. independent of the size of the laser spot. Although the Arrhenius damage integral adds up over the full duration where the tissue temperature is elevated, the main contribution to the damage integral comes from the higher temperatures during the pulse (as the cooling duration is in the millisecond regime). Thus, for pulse duration ranges from ms to s, the characteristic time for thermally induced damage is, in first approximation, the laser pulse duration. It follows that the breakpoint characterises the retinal spot radius which is (approximately) equal to the thermal diffusion distance for the respective pulse duration. The *in vitro* bovine and the computer model threshold data does not show an actual well defined sharp breakpoint between a 1/d dependence and no spot size dependence, but rather a smooth transition between the two regions, i.e. rather a 'knee' than a breakpoint. When a straight line is fitted in log-log space to the 1/d section of the curves and the intercept with the no-spot size dependence threshold level is considered as the breakpoint, then the breakpoint as function of pulse duration approximately exhibits the expected  $\sqrt{t}$  dependence for pulse durations between 0.1 ms and 1 s. It is noted that the *in vitro* bovine thresholds in the region left of the knee, for pulse durations of 1 ms and 10 ms, tend to be somewhat higher than the computer model thresholds, which are calculated for a minimal lesion diameter of 20  $\mu$ m. A possible explanation for this effect is that for most experimentally detected lesions, the lesion diameter is not 20  $\mu$ m but is larger, tending in size closer to the diameter of the laser beam. When the computer model uses a minimal lesion diameter which is the same size as the laser spot, rather than 20  $\mu$ m minimal lesion diameter, the calculated thresholds have a very similar tendency than the experimental thresholds. A similar spot size dependence was postulated for monkey thresholds in [12] where the slope was assumed to gradually decrease from -1 for longer pulse durations to 0 for shorter pulses. However, for setting exposure limits, it appears prudent to assume a minimal lesion diameter of about 20  $\mu$ m and thus consider the trend shown by the model data rather than the experimental data.

It is noted that the spot size dependence discussed in this paper relates to visible wavelengths only, and can be expected to be different for infrared wavelengths which penetrate more deeply into the choroid and where scattering also determines the effective exposure diameter. See [13] these proceedings for preliminary results on a variation of absorption coefficients.

#### 4.4 Time dependence

The threshold data can also be plotted as function of pulse duration for the range of retinal spot sizes to study their time dependence. The time dependence of the spot size dependence breakpoint also results in a variation of time dependence for the different retinal spot sizes which is currently not reflected in the MPEs. For a diameter of 23  $\mu$ m, the slope in log-log scaled time dependence is somewhat steeper than the value of 0.75 currently defined by the MPEs, it equals 0.9 for pulse durations longer than about 1 ms. For shorter pulse durations, the time dependence becomes shallower and according to the thermal model becomes zero (i.e. no time dependence) for pulse durations of less than about 10  $\mu$ s, which is also referred to as the thermal confinement region. The larger the spot size becomes, the more extends the region of shallower time dependence to longer times, so that for a spot size diameter of 2 mm, according to the model, the time dependence slope in log-log scale becomes 0.4. For pulse durations of less than about 0.1 ms, all the curves for the different spot sizes merge as they approach the thermal confinement region. An explanation of the experimentally

well established time dependence of  $t^{0.75}$  for monkey threshold data is that the monkey data is not really for the assumed small spot of 25  $\mu\text{m}$  but rather, as discussed in section 4.2, reflects the threshold of a larger spot of up to 100  $\mu\text{m}$  in diameter. For these spot sizes (being enlarged probably by intra-retinal scatter), the time dependence exponent would be somewhat reduced so that  $t^{0.75}$  would be a good fit for the experimental monkey data. Regarding the shallower time dependence for large spots, it can be noted that this is reminiscent of the time dependence of the MPEs for thermal corneal and skin damage, which is  $t^{0.25}$ . After all, these corneal and skin MPEs are based on threshold studies which used image diameters in order of millimetres, which would also exhibit a shallower time dependence than image sizes of less than 1 mm, relevant for retinal laser exposure. The thermal damage model predicts that under thermal confinement conditions, the thresholds in terms of energy per pulse (or radiant exposure per pulse) would no longer depend on the pulse duration. When the pulses become so short that heat flow during the pulse is negligible, the temperature rise within the tissue is governed by the heat capacity of the tissue and the energy absorbed within a certain volume of the tissue only. As the energy becomes deposited in the tissue, the temperature linearly increases up to the end of the pulse, when it reaches its maximum value, which is independent of the pulse duration and depends on the energy of the pulse only. Thus the temperature rise can easily be estimated by multiplying the radiant exposure with the absorption depth to obtain the energy deposited within the absorbing volume (assuming homogeneous absorption) and dividing this value by the heat capacity of the tissue. In the thermal confinement regime, the Arrhenius damage integral is governed by the cooling behaviour, which is long (in the millisecond regime) compared to the pulse duration.

#### 4.5 Limitation of the models

For longer pulse durations in the seconds time regime, the bovine model and the computer model are limited due to heat flow issues, such as missing blood flow and missing vitreous, as well as, for wavelengths in the blue and green region, due to photochemically induced damage that might have lower thresholds than thermally induced injuries. For pulse durations shorter than about 50  $\mu\text{s}$ , the application of the computer model to model thermal damage is limited since bubble formation and effects of ultrashort pulse exposure can not be modelled.

Porcine *in vitro* threshold experiments by Schüle et al. [23] distinguished between thermally induced damage and cell death where bubble formation around the melanosomes (microcavitation) could be detected. They decreased the pulse duration from 3 ms downwards and showed that for pulse durations of less than about 50  $\mu\text{s}$ , the damage mechanism at threshold level changes from a thermal one (that can well be modelled by the Arrhenius integral) to a damage mechanism which is based on the formation of microcavities (referred to also as ‘bubbles’) around the heavily absorbing melanosomes in the RPE, which reach relatively high temperatures (figure 9). Bubble induced *in vitro* threshold values are from several studies [23, 24, 25].

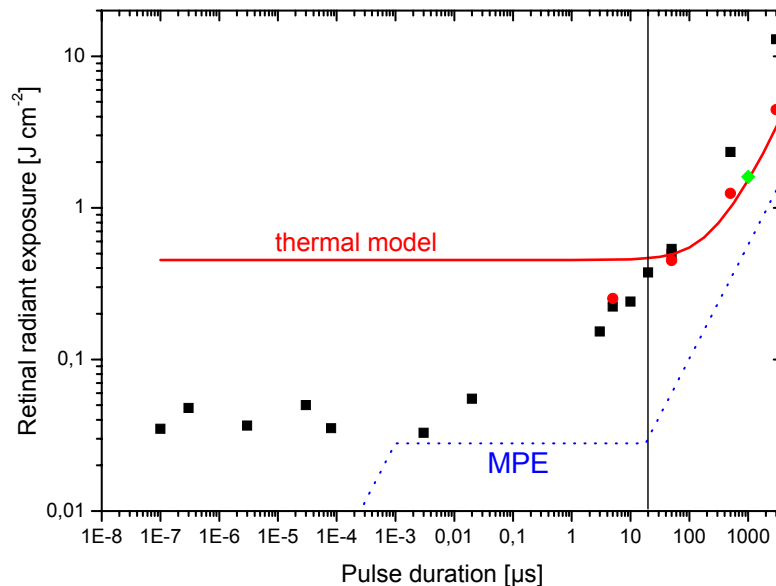


**Figure 9.** In vitro bubble induced damage thresholds from various sources (black squares) compared with thermally induced RPE cell damage in a porcine model (red circle), thermally induced RPE cell damage in bovine model (this work, green diamond) and thermal model.

The porcine *in vitro* thermal damage data given in [23] and shown figure 9 compares well with the bovine threshold and the computer model of this work, which is also plotted. It is important to note that the bubble induced threshold values continue to decrease for shorter pulse durations down to pulse durations of about 10 – 100 ns below which the bubble induced thresholds appear to remain constant. The factor between this lower threshold plateau and the thermal model threshold is about 10. The *in vitro* thresholds plotted in figure 9 also compare quite well with the 3  $\mu$ s and 7 ns Rhesus monkey data of Zuclich et al. [10], which explains the difference of the thermal model data with the 5 ns data of about factor 10. For the 3  $\mu$ s data, the bubble induced thresholds are not significantly lower than the thermally induced thresholds, according to the work of Schüle [23] and for this pulse duration, the thermal model is also a good fit for the monkey 3  $\mu$ s data of Zuclich [10], which therefore might be thermally induced or might be bubble induced damage. Computer models based on the Arrhenius integral can not model the absolute level of damage threshold for bubble induced injury, but for these conditions it can be assumed that the local radiant exposure level governs any spot size dependence. However, the bovine *in vitro* model still appears to be a viable alternative for animal experiments in the regime of bubble induced damage, i.e. for pulse durations down to the nanosecond regime.

## 5 CONCLUSIONS

Both the computer model and the bovine *in vitro* (explant) model presented here appear to be a good model for prediction of absolute levels of thermally induced damage thresholds in the pulse duration range of about 0.1 ms to 1 s in the visible wavelength range. For pulse durations less than approximately 50  $\mu$ s down to approximately 1 ns, thresholds seem to be determined by bubble formation around the melanosomes. In this time regime, the bovine *in vitro* (explant) model also appears to be applicable for absolute prediction of damage thresholds.

### 5.1 General safety factor

The computer model and the bovine *in vitro* model, for spot sizes less than about 80 - 100  $\mu$ s, predict a more conservative, i.e. lower threshold than can be observed for Rhesus monkey studies (figure 7). In section 4.2, two explanations are offered for the small spot - spot size dependence of Rhesus monkey threshold data, while we favour intra-retinal scattering as the correct explanation. The ‘safety factor’ of 10 that is often stated as general safety factor chosen by the committees setting laser exposure limits only applies to the minimal nominal laser spot sizes, for spot sizes above about 80  $\mu$ m - 100  $\mu$ m (5 - 6 mrad in the human standard eye) the safety factor in the millisecond pulse duration regime for green wavelengths is only a factor three. Compared to the often mentioned safety factor of 10, this might appear quite low. However, when the threshold values are determined with small experimental uncertainty and exhibit little spread by variability, which is the case for instance for the new 100 ms Rhesus monkey data and for the bovine *in vitro* data, then the dose response curve is quite sharp, close to a real step-function threshold, and the safety factor can be as small as three, while still assuring that at the MPE, no damage will occur (see also discussion in [5 and 26]).

At this stage it can not be ruled out that for nominal minimal retinal spot sizes, where MPEs tend to be a factor of 10 below experimental Rhesus monkey thresholds, RPE cell damage occurs at levels potentially only a factor of 3 above the MPE, at least in the fovea: if the explanation of intra-retinal scattering does apply, then this scattering would not occur in the fovea and for this condition, RPE cell damage appears possible for the minimal image size at a factor of about 3 above the current MPE, at least for heavily pigmented eyes. It appears that the choice of a safety factor of 10 for minimal images is a prudent one, since the actual threshold for an injury relevant on a medical and physiological level for vision is not certain but will most likely be somewhere between the levels predicted by the computer and *in vitro* bovine model and the levels determined in monkey *in vivo* experiments. Also the transfer of the results to the human case need to be done with caution – the impact of different pigmentation and racial differences for human exposure needs to be considered and might be different depending on pulse duration and image size. Without further detailed information, it might well be prudent to assume that the damage thresholds determined by the models discussed here would also apply in absolute terms for heavily pigmented human retinas. RPE pigmentation might not be that different for different races and differences in choroidal pigmentation might not play a significant role for shorter pulses.

### 5.2 Implications for Class 3R (Class IIIa)

The implications for the use of Class 3R (Class IIIa under current CDRH classification) lasers need to be further discussed. Experience for 30 years and tens of thousand of accidental exposures with 3 mW to 5 mW alignment lasers and laser pointers, show that unintentional exposures at levels up to five times above the MPE are safe. Retinal injuries were reported only for cases where somebody intentionally stared into the beam of such a product. However, we need to strongly warn against the conclusion from this that *all* Class 3R lasers are ‘safe’. This conclusion at the moment needs to be restricted to cw lasers which were classified based on the assumption of a minimal retinal spot, i.e.  $C_6$  (or  $C_E$  in ANSI) equal to unity (and since they are usually well collimated, the great majority of them really do produce a minimal nominal retinal spot). When extended source products are classified as Class 3R and the larger  $C_6$  is exploited, with a correspondingly output power higher than 5 mW, then the safety factor as discussed above would be only 3, and for nanosecond pulses and about 5 mrad apparent source size even less. Regarding the duration of exposure playing a role in the risk of such lasers, it is noted that due to the ‘shallow’ time dependence of the threshold and the limits when expressed as power or irradiance of  $t^{-0.25}$ , shorter exposure durations do not increase the safety factor significantly. For sources to be classified as extended source it is necessary that the divergence of the beam be at least as large as the value of  $\alpha$  that is used for determination of the limit (i.e.  $\alpha$  can never be less than the divergence of the beam [6, 7]). This means that the beam diameter does increase with distance to a greater extent than for small sources with a small divergence, so that at typical shorter range exposure distances of, say 0.5 or 1 m, a value of  $\alpha$  of for instance 10 mrad would necessarily result in a beam diameter of at least 5 mm to 10 mm, respectively. It follows that the practical exposure value approaches the worst case value based on a 7 mm pupil only for the case of a dilated pupil, i.e. only for conditions where the room is dark. The laser safety committees need to consider whether they restrict Class 3R lasers only to products which are classified based on the assumption of a small source, or whether Class 3R should be associated to some level of risk for retinal damage under certain conditions (dilated pupils, heavily pigmented eyes, depending on pulse duration). The latter would in practice create an uncertainty in the level of risk of Class 3R and would under a conservative simplified (but understandable) approach mean that all Class 3R laser products are considered to have this associated (if limited) risk, including those small divergence cw alignment lasers which by practical experience over 30 years were shown to be safe for responsible usage (i.e. for accidental exposure). Therefore, the authors would favour that Class 3R would in future revisions of the classification standards IEC 60825-1 and ANSI Z136.1 be restricted to the small source assumption ( $C_6 = 1$ ) only, which is currently the overwhelming majority of real products anyway.

### 5.3 Raising limits with time dependent $\alpha_{\max}$

The computer model and the bovine in vitro model show that there are unnecessarily high safety factor for short pulses and extended sources. This is due to the current constant  $\alpha_{\max}$  of 100 mrad, which in fact only applies to exposure durations in the seconds time regime. The breakpoint in the damage thresholds, which in meaning is equivalent to  $\alpha_{\max}$ , decreases for shorter exposure duration. This tendency can be observed in figures 10 for decreasing pulse duration from top left to bottom right.

Since the spot size dependence of the damage thresholds for pulse durations of less than about 0.1 ms goes with  $\alpha^2$  instead of the current  $\alpha$ , and the current  $\alpha_{\max}$  is fixed at 100 mrad, it follows that for short pulses, the safety factor could in principle be decreased by up to a factor of 66 for large sources (100 mrad/1.5 mrad). This would be accomplished by defining a time dependent value of  $\alpha_{\max}$ , where  $\alpha_{\max}$  equals 100 mrad at for instance 10 s, and decreases to 1.5 mrad at for instance 18  $\mu$ s (since 10 s and 18  $\mu$ s are already two anchoring points in the time dependence of the MPEs) as shown in figure 11, where in the right plot, the effect on the MPE is also shown.

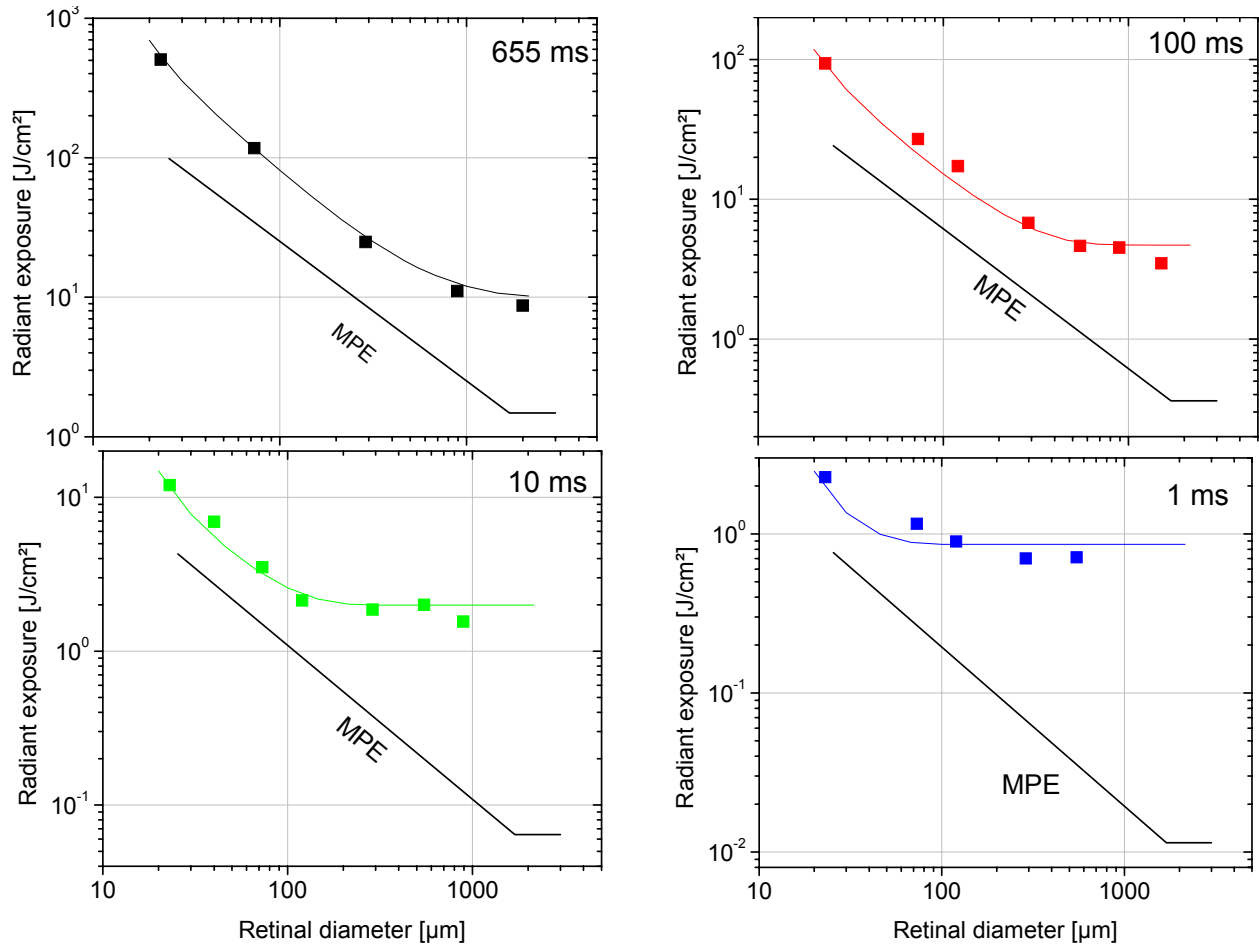


**Figure 10.** The current MPE values with  $\alpha_{\max}$  fixed at 100 mrad compared to damage thresholds determined in this work by a computer model (full line) and *in vitro* exposures of bovine retinas.

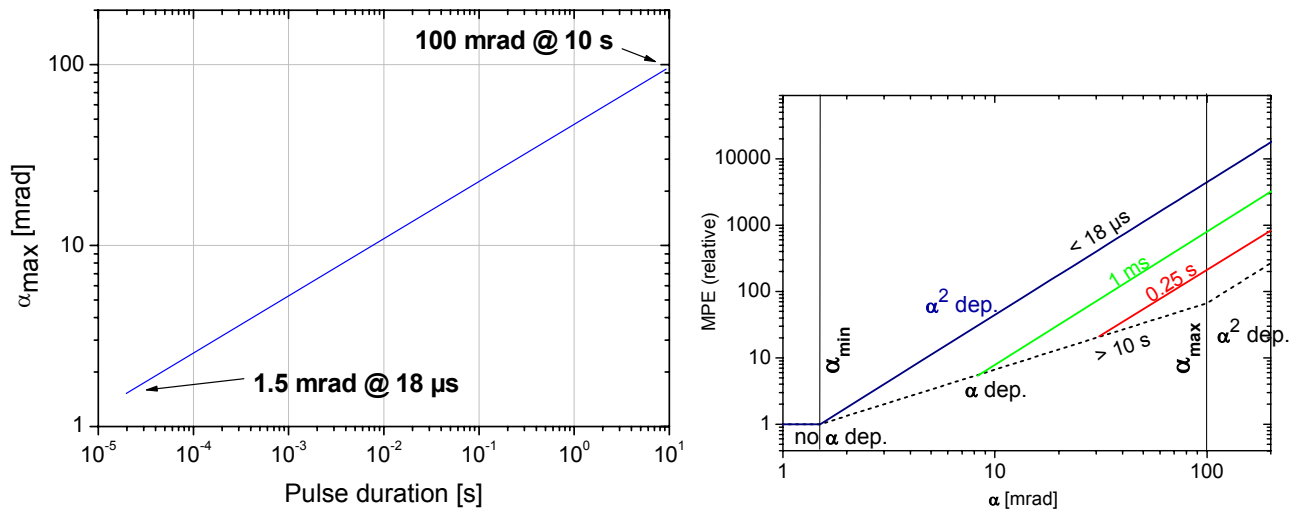


**Figure 11.** Left: Possible time dependence of a revised  $\alpha_{\max}$ . Right: Impact on MPEs for different pulse durations when  $\alpha_{\max}$  would become time dependent as indicated in the left plot.

Before the value of  $\alpha_{\max}$  can be made time dependent, the issue needs to be discussed also for wavelengths in the near infrared (i.e. up to 1400 nm) as well as how multiple pulses would need to be treated. Work on these issues is under way (see [13] this issue for preliminary results on modelling of the spot size dependence of near infrared wavelength radiation).

#### 5.4 Short pulse problem

The data of Zuclich et al. [10] has brought up a potential need to reduce the current MPEs so that the safety factor for the 7 ns pulse duration 80  $\mu\text{m}$  spot size threshold is raised to at least a level of 3, to make it comparable to the safety factor for other extended source MPEs. As shown in figure 9, this too small a safety factor seems to come about since the MPEs are held constant in terms of energy or radiant exposure for pulse durations less than 18  $\mu\text{s}$  (based on the thermal confinement regime of homogeneously absorbing media), while the damage thresholds, due to bubble formation which exhibits a lower threshold than thermally induced damage, continue to decrease. The current MPEs only decrease further for pulse durations less than 1 ns, to account for lower threshold in the ultrashort pulse duration regime [27]. Any lowering of the MPEs and AELs needs to be done with care and should be ideally done so that existing laser products are affected as little as possible, i.e. only for those conditions where the MPE (and therefore also the AEL for Class 1) was found to be too high. There are basically two possibilities to resolve this:

- 1) Increase  $\alpha_{\min}$
- 2) Decrease the MPE below about 50 ns with a different time dependence

On first examination of figure 2, an increase of  $\alpha_{\min}$  to a value of about 5 mrad (75 mrad) would establish the usual safety factor for the 5 ns threshold data, and with the proposed time dependent  $\alpha_{\max}$ , the MPEs for spot sizes larger than that would increase with  $\alpha^2$  and would keep a corresponding safety factor for all spot sizes. However, the big problem of this solution is that a change of  $\alpha_{\min}$  would affect all laser products that are classified based on a source size of between 1.5 mrad and the new  $\alpha_{\min}$ , where the emission limits and MPEs would be correspondingly lowered. It was shown in this work, that this is not necessary for pulse durations in the millisecond and second range and would unnecessarily lower the limits there, where quite a number of products already exist. We would therefore propose that it is considered to lower the limits for pulse durations starting at about 50 ns, either with an exponent for the time dependence appropriate so that the log-log line joins the current 1 ps MPE level (below which the MPE is again a constant radiant exposure value, i.e. independent on pulse duration), or introducing an additional plateau for the MPE between the current  $< 1\text{ps}$  and the current  $1\text{ ns} < t < 18\ \mu\text{s}$  plateau, so that the MPEs on either side of the plateau follow the 'usual'  $t^{0.75}$  dependency, i.e. would decrease left of the plateau with  $t^{0.75}$  equal to the current MPE values to meet the 1 ps level, and would increase right of the plateau with a  $t^{0.75}$  dependence to meet the current  $1\text{ ns} < t < 18\ \mu\text{s}$  plateau at 50 ns.

## 6 SUMMARY

An explant *in vitro* model based on freshly excised bovine retinas was developed to determine thermally induced damage thresholds. Thermal damage thresholds are predicted well by a computer model based on the Arrhenius integral. Both models, which are based on RPE induced damage, were validated against Rhesus monkey thresholds for wavelengths in the visible spectrum, particularly against new 100 ms threshold data.

Below pulse durations of about 50  $\mu\text{s}$ , bubble formation determines the damage threshold which can not be modeled with the present computer model. In the nanosecond pulse duration regime, thresholds reported in literature (*in vivo* and *in vitro*) are a factor of 10 lower than the thermal model would predict.

The *in vitro* bovine and computer model data show previously unknown spot size dependence where the breakpoint between the linear dependence on spot diameter and the region where the retinal threshold no longer depends on spot size depends on the pulse duration. This breakpoint could be adopted for a time dependent  $\alpha_{\max}$  in the exposure limits to reduce unnecessarily large safety factors.

An explanation based on intra-retinal scatter is offered for the unexpected spot size dependence for spot sizes less than about 80  $\mu\text{m}$ , experimentally observed for most Rhesus monkey threshold experiments. This scattering effect, however, would be strongly decreased or non-existent in the foveal pit, leading to lower thresholds there. The safety factor of 10 for minimal images when determined with Rhesus monkey studies therefore is prudent, since the actual threshold for RPE damage in the foveal pit might be a factor of three lower than the values reported in Rhesus monkey studies.

It was noted that the safety factor between the MPE and damage on RPE level in the monkey eye is only a factor of 3 for extended sources in the 100 ms regime (including 250 ms), and it is recommended that Class 3R as defined by IEC and ANSI laser safety standards is restricted to small source emission levels.

There is a need to lower the MPEs for 5 ns pulse duration, as an experimental threshold for a wavelength of 532 nm for 5 mrad angular subtense of the retinal image is basically equal to the current MPE. It is proposed to decrease the MPEs starting already at about 50 ns, not as currently is the case, at 1 ns.

### ACKNOWLEDGEMENTS

The authors would like to gratefully acknowledge frequent and fruitful discussions with David Sliney (US Army Center of Health Promotion and Medicine, Baltimore) and Bruce Stuck (US Army Research Detachment, San Antonio).

### REFERENCES

- [1] ICNIRP 1996 Guidelines on Limits for Laser Radiation of Wavelengths between 180 nm and 1,000  $\mu\text{m}$  *Health Physics* **71** 804-819
- ICNIRP 2000 Revision of guidelines on limits for laser radiation of wavelengths between 400 nm and 1.4  $\mu\text{m}$  *Health Physics* **79** 431-440
- [2] IEC 60825-1 Safety of laser products – Part 1: Equipment classification, requirements and user's guide, Ed 1.2, IEC Geneva August 2001
- [3] IEC 60825-14 Safety of laser products – Part 14: A users's guide
- [4] American National Standards institute (2000) American National Standard for the safe use of Lasers, Z136.1-2000. Orlando FL: Laser Institute of America.
- [5] Sliney DH, Mellerio J, Gabel VP, Schulmeister K. What is the meaning of threshold in laser injury experiments? Implications for human exposure limits. *Health Phys* 82(3):335-347, 2002
- [6] *Laser Safety*, Roy Henderson and Karl Schulmeister, IOPP Bristol and Philadelphia, 2004
- [7] Schulmeister K, 'The apparent source' – a multiple misnomer, ILSC 2005, ISBN 0-912035-79-X, Laser Institute of America, p. 91-98
- [8] Schulmeister K, Seiser B, Florian Edthofer, Grabner, Georg, Criteria for the determination of the 'thermal' retinal spot diameter, SPIE Proceedings Vol 5688B 2005, p 458 - 468.
- [9] Jacobson JH, Cooper B, Najac HW, Effects of thermal energy on retinal function, Report AMRL-TDR-62-96, 1962
- [10] Zuelich JA, Lund DJ, Edsall PR, Hollins RC, Smith PA, Stuck BE, McLin LN and Till S, 2000. Variation of laser-induced retinal damage threshold with retinal image size. *JLA* 12(2):74-80. 2000
- [11] Till S, Till J, Milsom PK, Rowlands G, A new model for laser induced thermal damage in the retina, *Bull Math Biol* 65: 731-746, 2003
- [12] Lund DJ., Schulmeister K, Seiser B, Edthofer F, Laser-induced retinal injury thresholds: Variation with retinal irradiated area SPIE Proceedings Vol 5688B, 2005, 469 - 478.
- [13] Schulmeister K. et al, to be submitted to *Journ Biomed Opt*
- [14] Lund DJ et al., to be submitted
- [15] Beatrice ES, Frisch GD. Retinal laser damage thresholds as a function of the image diameter. *Arch Environ Health* 27:322-326 1973
- [16] Ham WT Jr., Geeraets WT, Mueller HA, Williams RC, Clarke AM, Cleary SF. Retinal burn thresholds for the helium-neon laser in the rhesus monkey. *Arch Ophthalmol* 1970;84:797-809
- [17] Allen, R. G., Bruce, W. R., Kay, K. R., Morrison, L. K., Neish, R. A., Polaski, C. A., Richards, R. A., Research on Ocular Effects Produced by Thermal Radiation, "Final Report AF41(609) - 3099," Brooks AF Base, TX, AD 659146: (1967).
- [18] Maher EF, Transmission and absorption coefficients for ocular media of the rhesus monkey, USAF School of Aerospace Medicine Report SAM-TR-78-32, 1978

- [19] Alt C., Framme C, Schnell S, Brinkmann R, Lin, CP, Selective targeting of the retinal pigment epithelium using an acousto-optic laser scanner, *J Biomed Opt* 10, 064014 (2005).
- [20] Sliney D H and Wolbarsht M 1980 *Safety with Lasers and Other Optical Sources* (New York: Plenum Publishing Corp.)
- [21] Unterhuber A, Povazay B, Bizheva K, Advances in broad bandwidth light sources for ultrahigh resolution optical coherence tomography, *Phys. Med. Biol.* 49 (2004) 1235–1246
- [22] FDA, 21 CFR 1040 1994 *Performance standards for light-emitting products: Section 1040.10 Laser products and Section 1040.11 Specific purpose laser products* (Maryland: FDA)
- [23] Schüle G, Rumohr M, Hütmann, G and Brinkmann R, RPE damage thresholds and mechanisms for laser exposure in the microsecond to millisecond time regimen, *IOVS* 46, 714 – 719, 2005
- [24] DJ Payne, TR Jost, JJ Elliot, BE Eilert, L Lott, K Lott, GD Noojin, RA Hopkins JR, CP Lin, BA Rockwell Cavitation thresholds in the rabbit retina pigmented epithelium. *SPIE Vol 3601:27-31*, Jan 1999
- [25] Kelly MW. Intracellular cavitation as a mechanism of short-pulse laser injury to the retinal pigment epithelium. In: *Electrical Engineering: Tufts university*, 1997
- [26] Schulmeister K., Sonneck G., Hödlmoser H., Rattay F., Mellerio J. and Sliney D., Modeling of uncertainty associated with dose–response curves as applied for probabilistic risk assessment in laser safety *SPIE Vol. 4246*, *Proceedings of Laser and Noncoherent Light Ocular Effects: Epidemiology, Prevention, and Treatment III*, pp 155-172, San Jose 2001